Evolution of microstructure and mechanical properties in Cu–14%Fe alloy during severe cold rolling

N.D. Stepanov [a], A.V. Kuznetsov [a], G.A. Salishchev [a], N.E. Khlebova [b], V.I. Pantsyrny [b]

[a] Laboratory of Bulk Nanostructured Materials, Belgorod State University, Pobeda 85, Belgorod 308015, Russia
[b] LLC Scientific Production Company, NANOELECTRO, Rogova 5A, Moscow 123098, Russia

Keywords:
Microcomposite alloy
Cold rolling
Microstructure refinement
Supersaturated solid solution
Mechanical properties

A B S T R A C T

Cu–14%Fe alloy was produced by vacuum arc remelting and casting in water-cooled mold with subsequent hot extrusion. It had fine grained microstructure with supersaturated solid solutions based on Cu and Fe phases. The alloy was subjected to cold sheet rolling with true strains up to 6.6. Microstructure was studied by SEM and TEM, specific attention was paid to chemical composition of individual phases—copper matrix and iron particles. After rolling very fine lamellar structure formed in copper matrix. Rolling also has resulted in decrease of iron content in matrix from 3.8% in initial condition to 1% after rolling with strain of 5.1 due to decomposition of supersaturated solid solution. At higher strain some deformation-induced mechanical alloying was observed, leading to local increase of iron content. Iron particles also were heavily refined; their average thickness after rolling with strain of 6.6 is about 30 nm (according to TEM data). Several possible mechanisms of their refinement in addition to homogeneous plastic deformation are proposed. Strength of the alloy measured by tensile testing increased significantly after rolling. For example, ultimate tensile strength increased from 325 MPa in initial condition to almost 1000 MPa after rolling with strain of 6.6. Good correlation between mechanical strength and spacing between iron particles in accordance with Hall–Petch relationship was found.

1. Introduction

Copper-based microcomposite alloys are relatively new class of materials with high strength and high electroconductivity [1]. Such alloys are based on the systems like Cu–Ag, Cu–Nb, Cu–Fe of Cu–Cr, where second component has very low solubility in copper at room temperature and no intermetallic compounds form between components. The conductivity of copper matrix is not affected much by addition of alloying components because of their low solubility. Several techniques were developed to produce this kind of composites. So-called in situ composites are usually produced by casting ingot with desired composition with subsequent deformation [2,3]. During deformation with large strains the initial dendrites transform into fine particles. Strength of microcomposites increases with decrease in spacing between particles. Commonly microcomposites are drawn to very high strain levels, sometimes about or even more than 10 [4,5]. As a result very fine filaments of second component are formed. This treatment increases strength significantly, and strength level about 1 GPa or more can be achieved. Drawing of microcomposites was extensively studied. Alternative deformation scheme could be rolling with high strains. Rolling of copper-based microcomposites is much less studied than drawing. Most studies were performed for Cu–Nb [6,7] or Cu–Ag [8,9] alloys. It was shown that sheets or foils from microcomposite alloys can have comparable or even higher strength in comparison to wires after deformation with similar strain [10]. However, peculiarities of microstructure refinement and properties evolution during rolling still require additional studies.

Interesting phenomena, frequently found in microcomposite alloys, is formation of supersaturated solid solutions (ssss). Despite negligible solubility in copper of typical alloying components and vice versa, formation of ssss was reported for a number of alloy systems after heavy deformation [11]. Content of soluted element is often far beyond the equilibrium: for example, after high-pressure torsion at very high strains, iron was completely dissolved in copper matrix of Cu–15%Fe alloy [12]. But ssss could be found already in cast alloys if the cooling conditions are not equilibrium [13]. It is not clear how ssss present in as-cast condition would behave during extensive deformation, required to obtain fine structure and high strength.

Among all microcomposite alloy systems Cu–Fe is of particular interest because of low cost of iron [14]. However, solubility of iron in copper at room temperature is significantly higher than in other systems like Cu–Nb. Data on microstructure and properties

of Cu–Fe alloys after rolling is very limited [10]. The aim of current paper is to study the evolution of microstructure and mechanical properties of Cu–14%Fe alloy during rolling with high strains. Special emphasis would be made on chemical composition of individual phases.

2. Experimental procedures

Ingot of Cu–14.2(wt)%Fe (further referred as Cu–14%Fe alloy) alloy was prepared by double vacuum arc remelting and cast into water-cooled copper mold. Initial ingot with diameter 105 mm was extruded to rod with diameter 45 mm. Extrusion was performed at 650 °C. Prior to rolling rod was slightly forged at room temperature using hydraulic press in order to obtain plate with thickness about 25 mm. Rolling direction was kept perpendicular to extrusion direction. 2-Hi and 6-Hi rolling mills were used to produce sheets and foils with thickness from 1500 μm to 35 μm. Corresponding strains varied from 2.8 to 6.6.

Microstructure of sheets and foils was characterized with optical microscopy (Olympus GX51) and scanning electron microscopy (Quanta 2003D and Quanta 600 FEG, both equipped with EDS detector). Both transverse and longitudinal sections were analyzed. Several samples namely after rolling with strains of 3.7, 5.1 and 6.6 were subjected to more detailed study by TEM. Observations were performed on transverse section using JEOL JEM-2100. EDS analysis was used to identify Fe particles. For TEM samples preparation pieces of sheets/foils were glued into titanium cylinder having 3 mm in diameter with a cut inside. After that disks having thickness 0.2–0.3 mm were cut from this cylinder using Struers Accutom-5. Discs were mechanically grounded to 70–80 μm and then dimple grinded to achieve thickness in center 30–40 μm. Final thinning to obtain electron transparency was done by ion milling using Fishione ion mill. Ion milling was performed in two stages—first with accelerating voltage 6 kV and incidence angle 10° and second with 5 kV and 7°. Mechanical tests were performed with Instron 5882 testing machine. Gauge dimensions were 3 × 24 mm x samples thickness. All tests were performed at room temperature with initial strain rate $\sim 1 \times 10^3\ s^{-1}$.

3. Results

In extruded rod large both elongated and equiaxed Fe particles were observed with average thickness about 15 μm and average length 35 μm (Fig. 1a). SEM–EDS analysis revealed that these particles contained 10–12% of Cu. Average size of copper grains/subgrains was about 500 nm according to TEM data (Fig. 1b). Some nanoscale (with average size below 5 nm) Fe precipitates were found in copper matrix.

After rolling Fe particles were elongated in rolling direction (Fig. 2). Particles resembled either flattened lens or had planar geometry after rolling with moderate strains (Fig. 2a and b). Lens-like shape was more typical for transverse section; on longitudinal section particles were mostly elongated. After rolling with higher strain ($e \geq 5.1$) shape of the particles in longitudinal and transverse section becomes more uniform, however, some lens-like particles could be still found on transverse section (Fig. 2c and d). Significant variation of thickness along the length of some particles was observed. Many particles became subdivided by longitudinal layers of copper phase. After rolling with strain of ≥ 6 shape of the particles became rather uniform (Fig. 2e–h). It should be noted that difference between thickness of individual particles still remained very significant as it is clearly seen from comparison of images with different scales (Fig. 2e–h). However, difference in thickness along the axis of the particles became less prominent. Volume distribution of the particles was not homogeneous at all studied strains—areas almost not containing any particles coexisted with areas containing many particles.

Average thickness of the particles decreased with increase of strain (Fig. 3a). Thickness of particles decreased quite monotonically especially considering large scale of error bars. Final thickness after rolling with strain of 6.6 was about 0.2 μm. But even after highest strains both rather thin (with thickness down to 0.1 μm) and rather thick plates (thickness about 1–2 μm) could be found. This means that refinement of the particles happens inhomogeneously. Almost no difference in particles thickness between longitudinal and transverse sections could be found. Length of particles decreased like their thickness (Fig. 3b). Length could be underestimated because many of the particles were too long to fit into SEM image especially at low strains. Length of particles in transverse section is slightly smaller than in longitudinal section at low and moderate strains ($e \leq 5.5$). At high strains average length is equal in both sections. Minimal average length after rolling with $e=6.6$ is slightly more than 1 μm. Spacing between Fe particles decreases almost monotonically during of rolling (Fig. 3b). There was almost no difference of value of spacing between particles in longitudinal and transverse sections. Average spacing between the particles was about 0.4–0.5 μm after rolling with strain of 6.6.

TEM images of microstructure in longitudinal section are shown in Fig. 4. Structure of copper matrix transformed from relatively equiaxed one in initial condition (Fig. 1b) into elongated one with longitudinal boundaries being parallel to rolling plane.

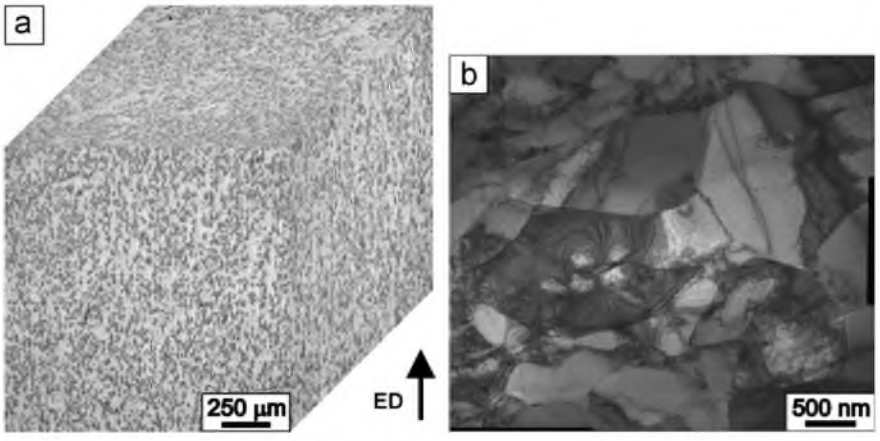

Fig. 1. Microstructure of initial Cu–14Fe alloy, (a) optical microscopy, extrusion direction is indicated by arrow, (b) TEM.

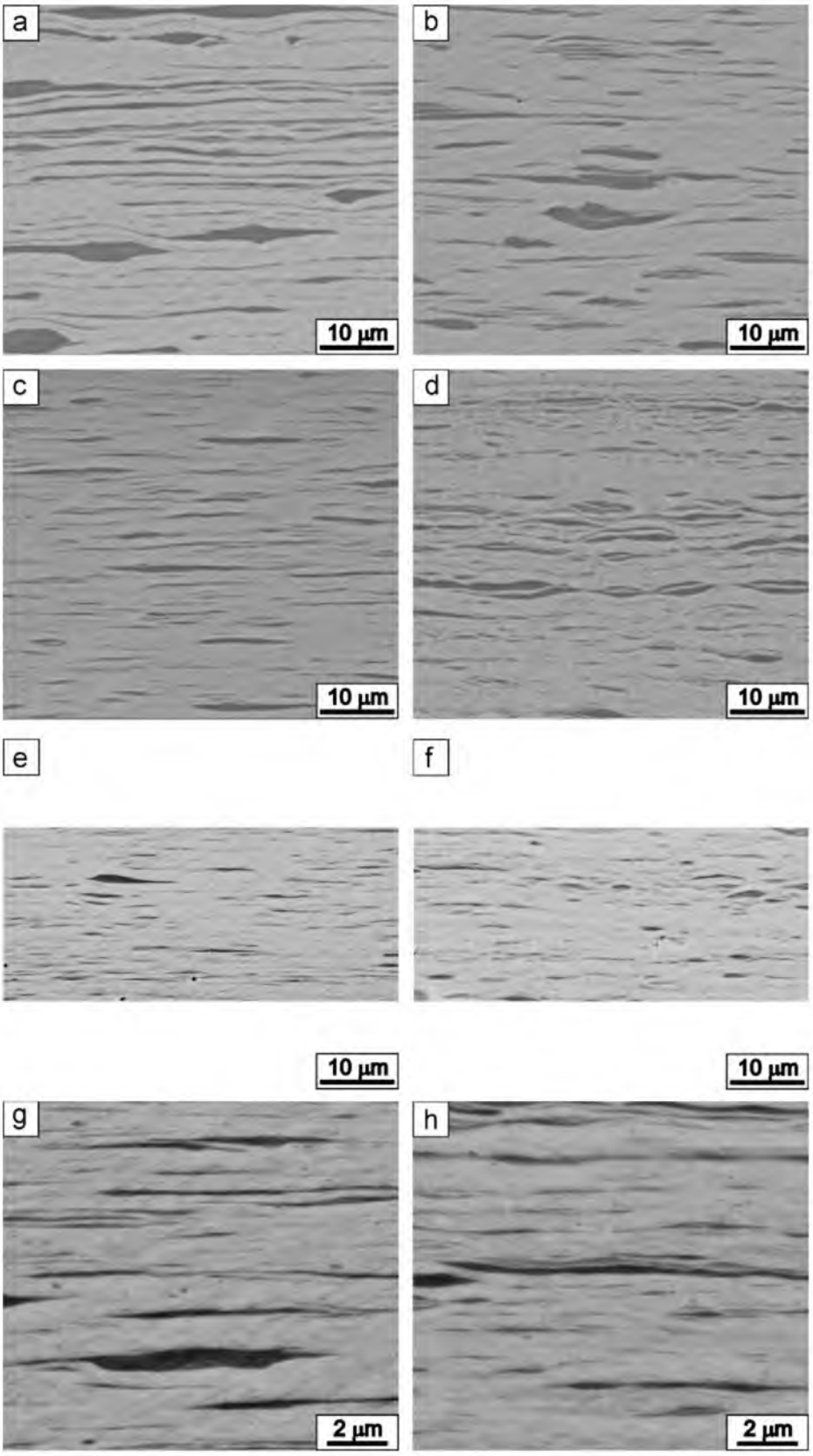

Fig. 2. Microstructure of Cu–14%Fe alloy after rolling at different strains, SEM images: (a), (b) $e=3.7$; (c), (d) $e=5.1$; (e), (f), (g), (h) $e=6.6$; (a), (c), (e), (g) longitudinal section, (b), (d), (f), (h) transversal section. Note that for $e=6.6$ two sets of images are shown: (e), (f) with the same resolution as the images for other strains and (g), (h) with higher magnification. Images with lower magnification have limited width due to small thickness of samples.

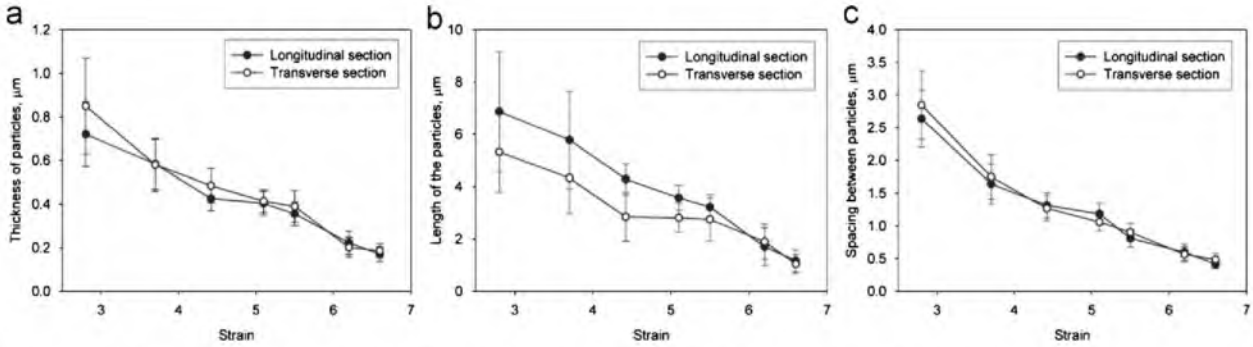

Fig. 3. Dependence of (a) average thickness and (b) average length of Fe particles, (c) average spacing between Fe particles on rolling strain, measured using SEM images.

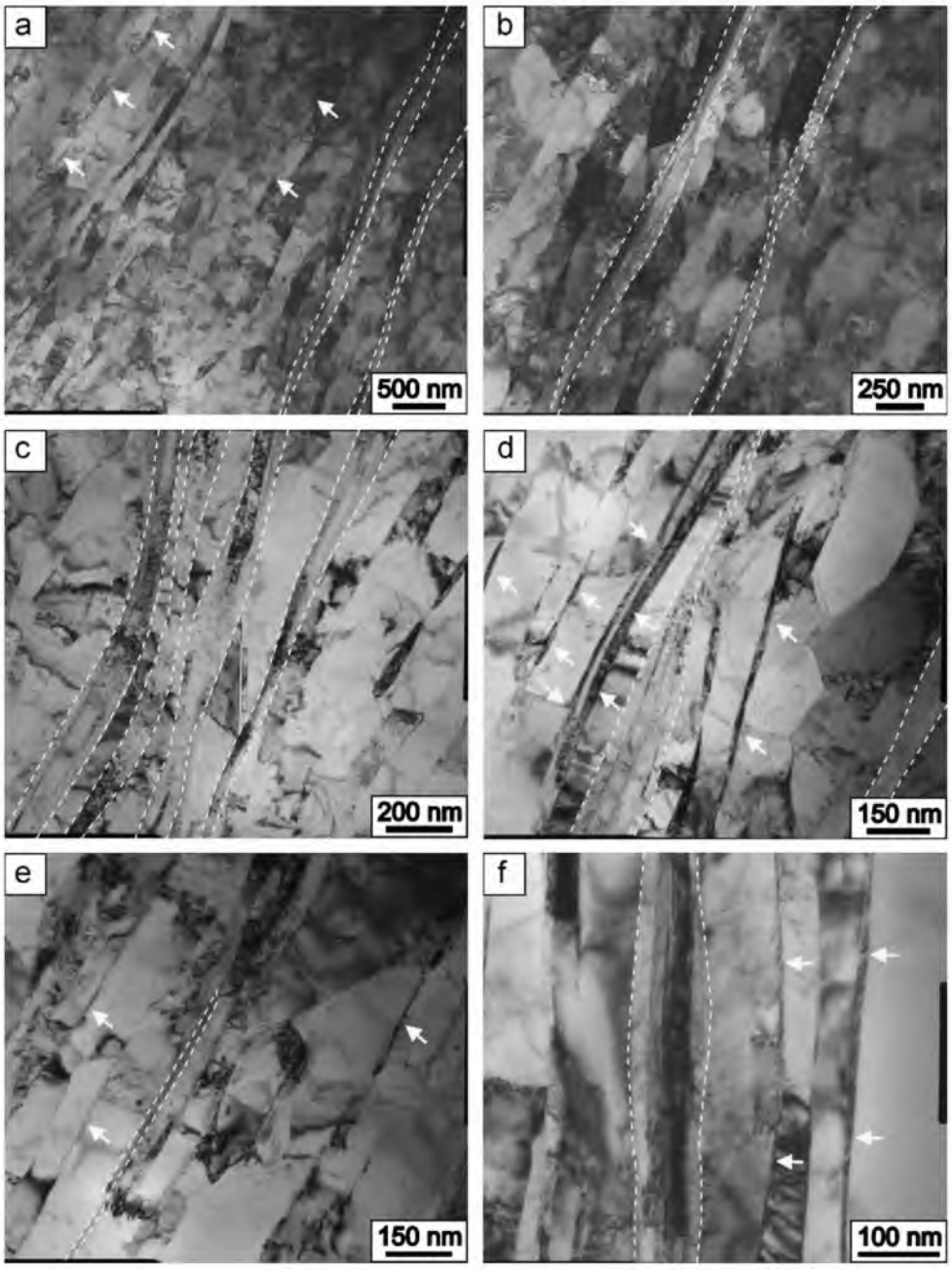

Fig. 4. Microstructure of Cu–14%Fe alloy after rolling with different strains, TEM images: (a), (b) $e=3.7$, (c), (d) $e=5.1$, (e), (f) $e=6.6$. Iron particles are indicated either by white dashed lines or by white arrows.

Increase of rolling strain results in refinement of the structure. Boundaries which were diffusively scattered after rolling with strain of 3.7 became sharper after additional straining.

Volume distribution of elongated iron particles (indicated by white arrows or highlighted by white dashed lines in Fig. 4) seems to be locally very inhomogeneous. The particles often tend to be located near each other, altogether with some areas containing only copper grains. This effect obviously is connected with the initial dendrite morphology of the Fe precipitates in as cast condition. During the extrusion process the transformation of the dendrite structure leads to rearrangement and alignment of the dendrite axes along the direction of extrusion. That is why the thickness of individual particles that could represent the initial dendrite's axes of different order significantly differs from one to another, and the difference could be as high as an order of magnitude. Some variations in thickness along the axis of particles was also found, typically for relatively thick ones with thickness exceeding a hundred of nm approximately, as well as local bending of the particles. Thin particles with thickness about several tens of nm were usually straight and had nearly constant thickness. It should be mentioned that particles with thickness above ~0.5 μm usually were not electron transparent after ion milling and so could not be characterized by TEM method. Interesting feature, not previously reported for copper-based in-situ composites, is presence of longitudinal boundaries inside some particles, generally relatively thick ones ($\geq$100 nm). Inter-boundary spacing is about several tens of nm. Increase of rolling strain results on refinement of iron particles, and after strain of 6.6 most of the particles is too fine to have longitudinal boundaries inside.

Quantitative outputs from TEM investigations are shown in Fig. 5. Copper matrix is characterized by transverse spacing of the boundaries (Fig.5a). Boundary spacing decreases gradually from 520 nm in extruded condition to 70 nm in 35-μm thickness foil. However, rate of structural refinement clearly diminishes at strains higher than 4. Similar tendency was found for distance between iron particles (Fig. 5b). No data is shown for initial sample as in this condition spacing was too large to be measured with TEM. Minimal measured average value is about 100 nm after rolling with strain of 6.6. Thickness of individual particles decreases monotonically, and reaches 30 nm after rolling strain of 6.6 (Fig. 5c).

TEM-EDS analysis of alloy in as-cast and extruded condition revealed very high content of iron in copper matrix—3.8(wt)%. Rolling results in gradual decrease of iron content down to 1.2% at strain equal to 5.1. However, further rolling does not result in any noticeable decrease of iron content. On the contrary, detailed observations of the foil rolled to maximum strain of 6.6 revealed that in areas near Fe particles iron content was significantly higher than in bulk of the specimen—about 2.4%. Also, as it was mentioned previously, in some copper grains numerous nanoscale spherical iron particles were found. Their mean size remained constant during rolling—about 3.5 nm, but volume fraction of copper grains, containing these nanoscale particles increased from about 7% in initial condition to 22% at strain of 5.1 (Fig. 6b). Further increase of strain had not resulted in significant increase of the volume fraction.

It was impossible to provide statistically reliable data on chemical composition of Fe particles as they mostly were too thin to measure chemical composition without being affected by surrounding copper matrix. However, it could be concluded that iron particles (relatively thick ones) contain about 5–10% of copper after rolling. Also the longitudinal boundaries inside particles seem to be significantly enriched with copper.

Evolution of mechanical properties during rolling is shown in Fig. 7. Strength values of initial rod (yield strength, Y.S. and ultimate tensile strength, U.T.S.) were 225 and 325 MPa, respectively and elongation to failure was 23%. Rolling resulted in obvious strengthening and loss of plasticity. Strength increased gradually with increase of strain up to $e \approx 4$. After that some kind of saturation is reached and strength rises only slightly as a result of rolling higher strains. U.T.S. value is in range of 680–770 MPa when strain changes from 4 to 5.5. But when rolling strain is more than 5.5 strength starts to rise rapidly again. Most significant strengthening was observed at $e \geq 6$. U.T.S. was found to be equal to 869 and 993 MPa, and Y.S. was about 780 and 880 MPa at strains equal to 6.2 and 6.6, respectively. Elongation showed opposite behavior to strength. It decreases significantly at low strains ($e \leq 4$). Further increase of strain up to 5.5 resulted in slight reduce of elongation in range 5–8%. Significant strengthening at $e \geq 6$ was accompanied by drop of elongation to approximately 2%.

4. Discussion

It is well established fact that copper-based in situ micro-composites are based on systems with negligible solubility of both components. However, from the data given above, it is clear that microstructure of the studied Cu–14Fe alloy consists from two solid solutions, namely Cu (matrix)- and Fe (particles)- based. Both of the solid solutions are heavily supersaturated. This could not be expected from equilibrium phase diagram, but it was demonstrated that it is possible to obtain solid solutions in alloys between immiscible elements by various non-equilibrium processes [15], including rapid quenching [13]. Rolling not only

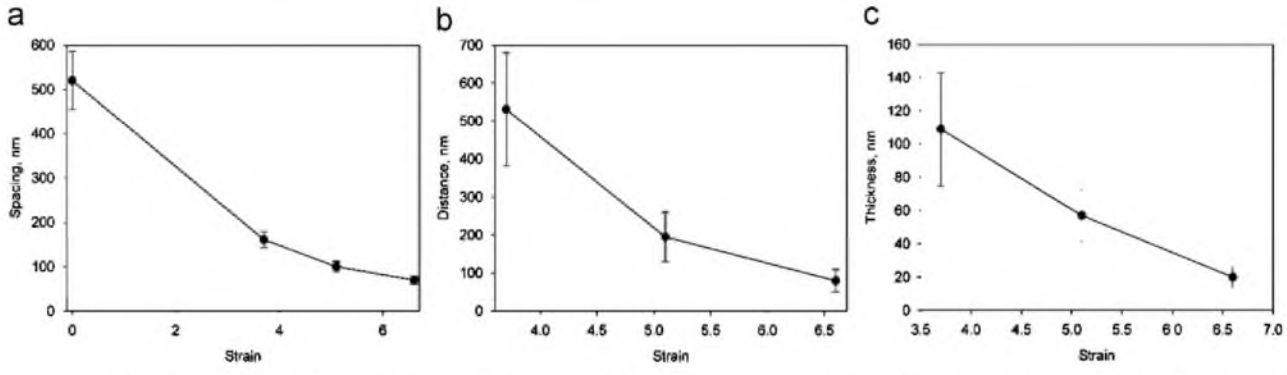

Fig. 5. Dependence of (a) spacing between longitudinal boundaries in copper matrix, (b) distance between Fe particles, and (c) thickness of Fe particles on rolling strain, measured using TEM images.

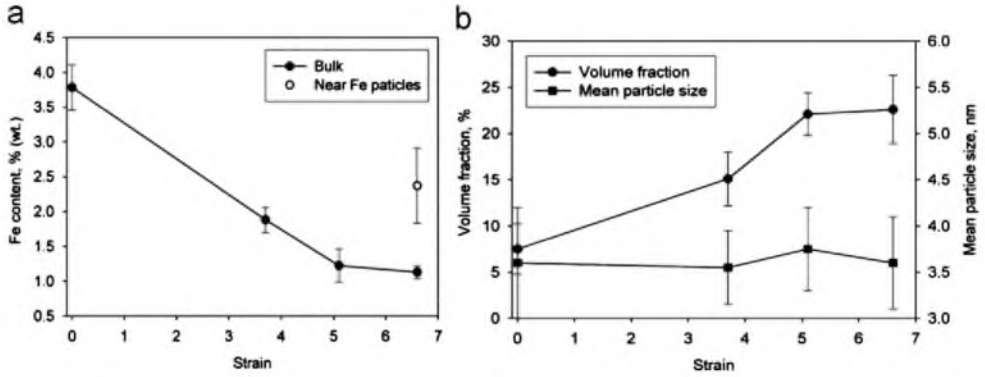

Fig. 6. Dependence of (a) Fe content in copper matrix (measured by TEM-EDS) and (b) volume fraction of grain/subgrains containing Fe precipitates and average size of these precipitates, on rolling strain.

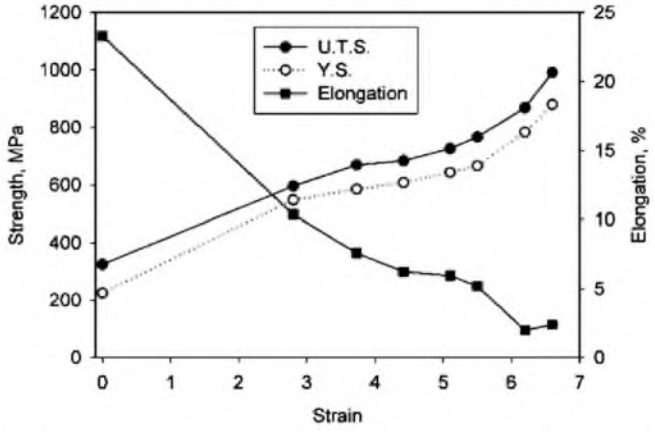

Fig. 7. Dependence of mechanical properties of Cu–14%Fe alloy after rolling on strain.

induces significant refinement of both phases resulting in noticeable increase of strength, but also changes composition of the phases. Peculiarities of microstructure evolution during rolling would be analyzed below, as well as mechanical properties and their correlation with microstructure.

4.1. *Cu-based solid solution*

Cu-based solid solution is the matrix phase of the Cu–14%Fe alloy. The matrix has a fine-grained microstructure with mean grain size of 0.5 μm already in initial extruded condition. Rolling transforms microstructure of copper matrix into lamellar one and significantly refines it. Spacing between lamellar boundaries is as fine as 70 nm after rolling with strain of 6.6. Lamellar structure is typical for heavily rolled pure metals [16]. However, several differences from structure of cold-rolled copper [17] could be mentioned. First, the grains/subgrains have relatively low aspect ratio. This could be attributed to pronounced dynamic recrystallization, considered as a common feature of copper-based microcomposite alloys [6]. Indeed, many grains with sharp straight boundaries could be found on TEM images, especially after large strains. These should develop as a result of dynamic recrystallization. Second, size of grains/subgrains is smaller than in pure copper. Fine size of structural elements is surely related with presence of iron particles. Microstructure development in copper matrix was widely studied, for instance for Cu–Fe alloy after drawing [18] and for Cu–Nb alloy after rolling [6]. Much less addressed topic is change in chemical composition of phases during deformation processing of microcomposite alloys. So, further we are going to focus on evolution of chemical composition of copper matrix during rolling.

The value of measured Fe content of 3.8% in copper-based solid solution in initial extruded condition is in great contrast with almost zero equilibrium solubility at room temperature (0.02(wt)%) [19]. Such ssss could not form during extrusion process as at the temperature of extrusion (650 °C) equilibrium solubility of iron in copper is still more than two times lower than measured one, so high content of iron is likely to come from casting procedure. It should be noted that solidification process in microcomposite copper-based alloys is a complex process, largely depending on both condition of the process conditions and the alloy composition [13,20]. It was shown that in certain conditions (at cooling rates from 10 K/s up to 100–200 K/s) it is possible to obtain structures, consisting from heavily supersaturated solid solutions [20]. However, abovementioned results were obtained for small laboratory-scale samples produced by special casting techniques. There is some lack of data on content of second element in copper for conventionally cast in-situ composites, but for Cu–8%Fe alloy content of iron in matrix of about 4.4 wt% was reported [21]. Precipitation of secondary Fe particles after annealing treatment of cast Cu–Fe alloys [22] was also found. In the current study, alloy was produced using industrial scale equipment and cast into water-cooled mold which ensured high cooling rate. It is difficult to precisely determine value of cooling rate due to complex nature of the process, but rough estimation gives a value of ≈ 5 K/s. It should be noted that at the initial stages of cooling when the temperatures are high and so are diffusion rates the cooling rates are expected to be much higher—at least an order of magnitude higher than the abovementioned ones. Such a high cooling rate seems to be enough to fix the concentration of Fe approximately equal to the maximum 4.4 wt% content in a solid solution at 1000 °C. So it is possible that the Cu–Fe alloy during the deformation has non-equilibrium composition with ssss formed already after casting.

Rolling with moderate strains ($3 \leq e \leq 5.5$) results in decrease of iron content down to 1.2%. Also volume fraction of copper grains containing nanoscale Fe precipitates increases from 7% in initial state to 22%. These facts indicate decomposition of ssss resulting in precipitation of Fe. It is well known that deformation produces lattice defects, such as vacancies, dislocations or grain boundaries. These defects could stimulate precipitation from ssss in two ways. First, they enhance diffusion rate in bulk material, and second they could serve as a preferred places for particle nucleation. In Al–Zn [23] and Cu–Ni [24] alloys ssss formed after casting was reported to decompose after high-pressure torsion, i.e., process involving very high strain level at room temperature. However, it is worth to note that in aluminum alloy authors proposed that main mechanism responsible for decomposition

was grain boundary diffusion, and particles of Zn were clearly located on grain boundaries. In our case particles were located inside grains. Similarly, nanoscale particles of Nb inside copper grains were found in Cu–Nb microcomposites in this case Nb could dissolve in matrix during high temperature processing and precipitate during annealing between drawing passes [25]. So it might be suggested that grain boundary diffusion is less important for ssss decomposition in copper-based microcomposites, and it is controlled either by bulk diffusion (accelerated by generation of vacancies) or pipe diffusion (accelerated by dislocations).

However, at higher strains of ≥ 5.5 Fe content is nearly constant, about 1% and at regions near Fe particles the content was even higher, about 3%. Also volume fraction of copper grains with Fe precipitates remains almost unchanged. It indicates less active decomposition of ssss. Higher content near Fe particles should be due to mechanical alloying of particles and copper matrix during deformation. This phenomenon, leading to formation of ssss, was often reported in heavily deformed copper-based microcomposites, including Cu–Fe [12] and Cu–Ag–Nb [26]. Several possible mechanisms of ssss formation during cold working were proposed, comprehensive overview of them was recently given in [11]. However, it is clear that interphase boundaries have a crucial role in this process so there is no surprise that higher iron content was measured near the iron particles.

As a summary, during cold rolling of Cu–14Fe alloy two competitive processes both effecting Fe content in Cu-based solid solution occur: decomposition of initial Cu-based ssss and mechanical alloying between matrix and iron particles. Their effect on Fe content is opposite, increase and decrease of it respectively. Rate of ssss decomposition is directly related to Fe content, so it would be more pronounced at initial stages of deformation, when the content is high, and will become less active at higher strains due to decrease of Fe concentration. Mechanical alloying is controlled by diffusion across interphase boundaries and thus is more active at high strains when the particles are heavily refined and area of interphase boundaries is high. So, the resulting Fe content should come from interaction of these processes. At the earlier stages of deformation, Fe content decreases due to decomposition of ssss. After that, saturation stage with constant Fe content is reached as decomposition becomes slower, and mechanical alloying begins. Increase of Fe content is anticipated in this case and it was indeed found, but only at areas near Fe particles. It could be hypothesized that at higher strains than achieved in this study we would observe more pronounced increase of Fe content in Cu-based solid solution.

4.2. *Refinement of Fe-based particles*

Iron particles have shape of coarse cylinders with diameter of $\sim$15 μm and height of $\sim$35 μm in initial cast and extruded condition. After rolling the particles change their shape to planar and become aligned with rolling plane. Their dimensions decrease significantly, and TEM indicate presence of many particles with thickness as low as several tens of nm. However, some relatively coarse particles with thickness of about several μm were found even after rolling with the highest strain. Similar appearance of Nb particles was reported for rolled Cu–20%Nb alloy [6]. However, mechanisms of refinement of second phase particles in Cu-based microcomposite alloys especially during rolling have not been described much. From a simplified point of view, the particles should change their shape in accordance with overall specimen shape change if they are homogeneously deformed plastically. However, our measurements have demonstrated that both length and thickness of particles decreases. It clearly indicates that particles do not only deform plastically but also undergo fracture during rolling. Fracture of particles during rolling also could be the reason of the significant difference in sizes between individual particles. The possible mechanisms of deformation-induced refinement of the particles in addition to plastic deformation are briefly discussed below.

From the SEM images it is seen that plastic deformation of the particles occurs seemingly non homogeneous. Thickness of individual particle could significantly vary along its axis. Several reasons could be responsible for inhomogeneous thinning of the particles. First of all, the cylinder-shaped particles have inhomogeneous thickness already in initial as-cast and extruded conditions—central part is thicker than the periphery. The second important factor is associated with the difference in crystallographic orientation of the particular particles that were initially formed as free crystallized dendrites statistically dispersed in a copper matrix. It could be also expected that the peripheral parts of needle form particles (former dendrite' axes) would deform easier as they have lower thickness and thus lower stresses are required for plastic deformation. SEM images especially after rolling with relatively low strains (Fig. 2a and b) clearly demonstrate particles which have shape of lens—thick central part and very thin edges. This type of morphology could be developed through thinning of peripheral parts of initial particles. One more feature of inhomogeneous deformation is local "necking" of some of the particles, which became very thin in one or several specific points. It might be assumed that "necking" is related with composite nature of studied material. Copper-based matrix is more plastic than iron particles and thus deforms easier. Thus homogeneous deformation of iron particles does not allow maintaining strain compatibility with copper matrix. Development of "necking" ensures sufficient strain compatibility between iron particles and copper matrix, impossible with homogeneous deformation of the particles. Final stage of "necking" is complete fracture of the particle into two separate pieces. Due to fracture of the particles their average length decreases contrary to increase of their length anticipated in case of homogeneous deformation.

Due to thinning of the peripheral parts and "necking" some areas of the particles remain relatively thick. However, the SEM images demonstrate that these thick areas also are refined through the rolling process. It was also observed that the iron particles in some areas were very closely spaced looking as to be subdivided by copper layers aligned parallel with rolling plane. Usually a set of iron particles were subdivided by several layers simultaneously, thus forming several particles with the length of initial one and smaller thickness. This kind of behavior could not be anticipated from any mechanical considerations. However, TEM images showcase presence of longitudinal boundaries inside iron particles. These boundaries may be deformation-induced geometrically necessary boundaries, developed during rolling. They are aligned parallel with rolling plane, similarly to above-mentioned copper layers. Moreover, TEM-EDS analysis demonstrates that at least some of these boundaries are enriched with copper. Image of one of the iron particles with selected area diffraction pattern (SAED) taken from the particle is shown in Fig. 8. On SAED reflex from copper is seen, indicating that possibly some amount of copper phase is present inside the iron particle. It may be suggested that the copper phase is formed on the longitudinal boundaries inside the particles, as they are enriched with it. It was mentioned earlier that in initial as-cast and extruded condition content of copper in iron particles is about 11–12% (according to SEM–EDS analysis). This content significantly exceeds equilibrium solubility of iron in copper at room temperature, and as it was mentioned previously, most possibly is related with non-equilibrium cooling conditions during casting. So, it may be expected that during deformation copper would

segregate on developing longitudinal boundaries as they are thermodynamically preferred cites for segregations [27]. These segregations form layers of copper phase inside iron particles. It seems that development of these layers due to continuous segregation of copper from iron particles and possibly due to interaction with copper matrix leads to "lamination" of particle, leading to substantial refinement.

4.3. Mechanical properties

Possibility of obtaining high strength after high strain processing is maybe the most attractive feature of microcomposite copper-based alloys. Most commonly microcomposites are processed by drawing, so there is no lack in data on strength of microcomposite alloys, including Cu–Fe system alloys after drawing. Data on rolled microcomposites is limited mainly to Cu–Nb system alloys. The dependence between processing strain and U.T.S. is shown in Fig. 9: for various drawn Cu–Fe alloys in Fig. 9a, for various rolled Cu–Nb-based alloys in Fig. 9b. It should be noted that alloys had not only different compositions but also were prepared by different means (ingot metallurgy, powder metallurgy) and had different microstructure (initial size of Fe particles). Data on Cu–14%Fe alloy (current research) is indicated with thick solid line. The dependences of strength on processing strain were different, but some common features could be mentioned. Non-monotonical dependence of strength on strain was typical for nearly all the alloys. The most rapid increase of strength was found after high processing strain; however the values of the "high strain" differed a lot for each alloy. Results obtained in current study have similar features. Three stages could be distinguished. On the first stage strength (U.T.S.) increases gradually from 325 MPa in initial extruded rod to about 680 MPa after rolling at $e=4$. Slight increase of strength approximately from 680 to 770 MPa is observed at second stage ($4 \le e \le 5.5$). And finally most significant strengthening up to almost 1 GPa was observed at third stage ($e \ge 5.5$). Strength of cold-rolled Cu–14%Fe microcomposite alloy is comparable to strength of drawn alloys of this system (Fig. 9a) at given strain, so rolling and drawing seem to have similar strengthening effect on microcomposite alloys. It should be noted that no overall correlation between composition of the alloy and its strength was found. Alloys with higher Fe (Nb) content could be expected to have higher strength, but the Fig. 9 disproves this suggestion. Most possibly initial microstructure is more important for development of strength, than chemical composition. From Fig. 8b it is clearly seen that Cu–14%Fe alloy has same of higher strength than cold rolled Cu–Nb based alloys. Similarly, strength of Cu–20%Fe was found to be higher than strength of Cu–20%Nb (both alloys were produced by powder metallurgy) [6]. This fact was attributed to the difference in shear modulus of iron and niobium. Shear modulus of iron is twice higher than niobium's (81.6 versus 37.5 MPa) and iron particles strengthen copper matrix more effectively than niobium. Possibly this is the reason of higher strength of Cu–Fe alloy.

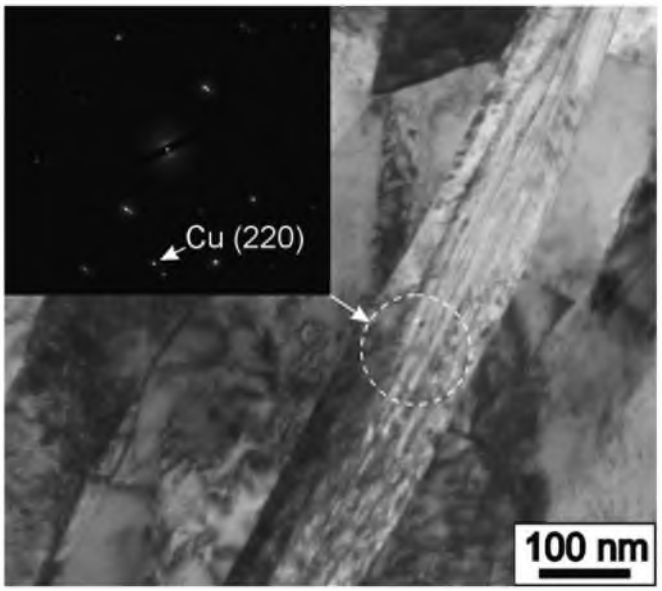

Fig. 8. TEM image of the rolled alloy ($e=3.7$) with SAED pattern from highlighted area. Reflex from copper lattice on SAED pattern is highlighted.

Strength of microcomposite copper-based alloys is often correlated with particles spacing using Hall–Petch relationship:

$$\text{U.T.S.} = \sigma_0 + \text{kx}\lambda^{-1/2}$$

where σ_0 is the stress required to move dislocations in the matrix and the particles and λ is spacing between particles. This correlation works well for drawn Cu–Fe alloys. Fig. 10 shows Hall–Petch type for rolled Cu–14%Fe alloy (SEM data for particles spacing was used). It is clearly seen that good correlation between experimental data and values predicted by the following expression was found:

$$\text{U.T.S.} = 318.8 + 433.5\text{x}\lambda^{-1/2}$$

In this equation $\sigma_0 = 318.8$ is very close to the strength of the initial extruded rod (325 MPa). It seems rather reasonable because coarse slightly elongated iron particles in as-extruded rod are unlikely to produce significant strengthening. The value $k = 433.5$ MPa/$\mu m^{-1/2}$ is significantly lower than the one measured for drawn Cu–Fe alloys—1319 MPa/$\mu m^{-1/2}$ for Cu–12%Fe

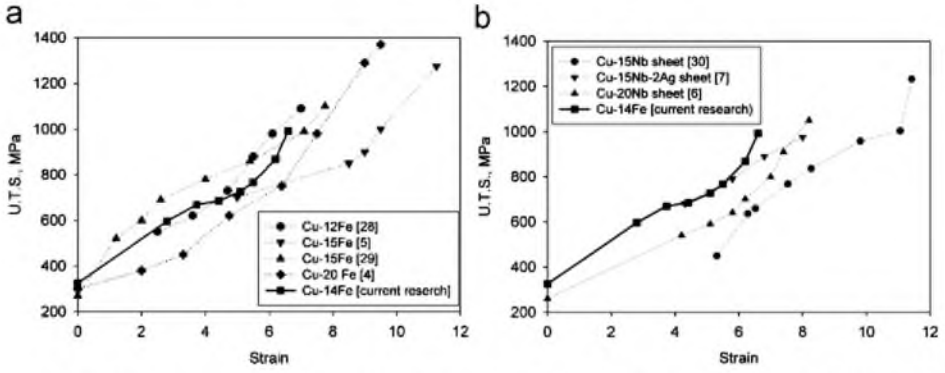

Fig. 9. U.T.S. – processing strain relationship for (a) – drawing of various Cu–Fe alloys, (b) – rolling of various Cu–Nb alloys; data for Cu–14%Fe alloy used in current study is indicated with solid line.

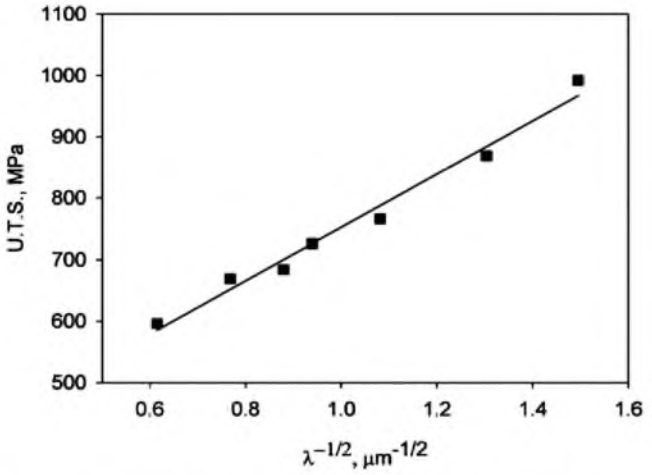

Fig. 10. Hall–Petch type relationship between U.T.S. and Fe particles spacing for Cu–14%Fe alloy after rolling.

alloy [26] and 1230–1550 MPa/$\mu m^{-1/2}$ for different Cu–20% Fe alloys [4]. Comparison between rolled and drawn Cu–20%Nb alloy has revealed similar phenomena—k value was about three times higher in case of drawn alloy (300 MPa/$\mu m^{-1/2}$ and 1000 MPa/$\mu m^{-1/2}$ for rolled and drawn alloy, respectively) [6]. The reason for such discrepancy between strengthening coefficients from second phase particles after rolling and drawing could be found in their morphology [31]. After rolling the particles obtain planar geometry and became aligned parallel with sheet surface. After drawing particles resemble kinked elongated ribbons. They are parallel to the axis of the wire but could be variously rotated around it. As the ribbons after drawing are not aligned with one specific plane as the particles after rolling they could be more effective as obstacles for dislocations. This has to be the reason why the strengthening coefficient is significantly lower after rolling.

However, despite higher k after drawing, strength of rolled Cu–14%Fe alloy was similar to the strength of drawn alloys at given processing strains (see Fig. 9a). The same was found for rolled Cu–20%Nb composite [6]. In case of Cu–Nb alloy it was attributed to the finer spacing between Nb filaments after rolling. Similar behavior is highly anticipated in Cu–Fe alloys. Indeed, from data available in [4] and [28] it is possible to calculate average spacing between filaments for Cu–20%Fe and Cu–12%Fe alloys. It was about 3 μm at strain approximately equal to 7. From our data (Fig. 3c) it is seen that average spacing between particles was about 0.4–0.5 μm at $e=6.6$. So the spacing between the particles is almost an order of magnitude lower in case of rolling. May be finer particle spacing after rolling is due to processes of particles refinement described earlier.

5. Conclusions

In this work hot extruded rods from Cu–14Fe alloy were cold-rolled with true strains of up to 6.6. Microstructural characterization and mechanical testing have shown the following:

1) Rolling resulted in significant microstructural refinement of the Cu–14%Fe alloy. Both copper matrix and iron particles were heavily refined, average boundary spacing of 70 nm in copper matrix and average iron particle thickness of 30 nm was reached after rolling with strain of 6.6 according to TEM data.
2) Copper matrix was significantly supersaturated with iron (3.8%) in initial as-cast and extruded condition. Rolling has promoted changes in chemical composition of copper matrix. At the initial stages of rolling, decomposition of supersaturated solid solution occurred and numerous nanoscale (average size about 3.5 nm) iron precipitates appeared. After rolling with strain of ≥ 5 iron content stabilized at approximately 1%. Deformation-induced mechanical alloying was found after rolling with strain of 6.6.
3) Significant strengthening was observed after rolling, maximum obtained U.T.S. was about 1 GPa after rolling with strain of 6.6. Good correlation between strength and iron particle spacing according to Hall–Petch relationship was found.

Acknowledgments

Authors would like to thank V. Drobyshev and N. Gudinova (Nanoelectro) who participated in preparation of the initial ingots and S. Sudiev (Nanoelectro) for valuable discussions. This work was supported by Russian Ministry of Science and Education through Federal program "Scientific and educational personnel for innovative Russia".

References

[1] F. Heringhaus, D. Raabe, J. Mater. Process. Technol. 59 (1996) 367–372.
[2] J.D. Verhoeven, E.D. Gibson, F.A. Schmidt, D.K. Finnemore, J. Mater. Sci. 15 (1980) 1449–1455.
[3] W.A. Spitzig, H.L. Downing, F.C. Laabs, E.D. Gibson, J.D. Verhoeven, Metall. Trans. A 24 (1993) 7–14.
[4] Y.S. Go, W.A. Spitzig, J. Mater. Sci. 26 (1991) 163–171.
[5] G.A. Jerman, I.E. Anderson, J.D. Verhoeven, Metall. Trans. A 24 (1993) 35–42.
[6] C.L. Trybus, W.A. Spitzig, Acta Metall. 37 (7) (1989) 1971–1981.
[7] J.D. Verhoeven, W.A. Spitzig, L.L. Jones, H.L. Downing, C.L. Trybus, E.D. Gibson, L.S. Chumnley, L.G. Fritzemeier, G.D. Schnittgrund, J. Mater. Eng. Perform. 12 (1990) 127–139.
[8] M.S. Lim, J.S. Song, S.I. Hong, J. Mater. Sci. 35 (2000) 4557–4561.
[9] W.-B. Lee, E.-N. Yoon, S.-B. Jung, J. Mater. Sci. Lett. 22 (2003) 1751–1754.
[10] J.S. Song, J.H. Ahn, H.S. Kim, S.I. Hong, J. Mater. Sci. 36 (2001) 5881–5884.
[11] D. Raabe, P.-P. Choi, Y. Li, A. Kostka, X. Sauvage, F. Lecouturier, K. Hono, R. Kirchheim, R. Pippan, D. Embury, Mater. Res. Bull. 35 (2010) 982–990.
[12] X. Quelennec, A. Menand, J.M. Le Breton, R. Pippan, X. Sauvage, Phil. Mag. 90 (9) (2010) 1179–1195.
[13] A. Munitz, A. Venkert, P. Landau, M.J. Kaufman, R. Abbaschian, J. Mater. Sci. 47 (2012) 7955–7970.
[14] J.D. Verhoeven, S.C. Chueh, E.D. Gibson, J. Mater. Sci. 24 (1989) 1748–1752.
[15] E. Ma, Prog. Mater. Sci. 50 (2005) 413–509.
[16] D.A. Hughes, N. Hansen, Acta Mater 48 (2000) 2985–3004.
[17] N.D. Stepanov, A.V. Kuznetsov, G.A. Salishchev, G.I. Raab, R.Z. Valiev, Mater. Sci. Eng. A. 554 (2012) 105–115.
[18] C. Biselli, D.G. Morris, Acta Mater. 44 (2) (1994) 493–504.
[19] A.G.H. Anderson, A.W. Kingsburu, Trans. AIME 152 (1993) 38–47.
[20] A. Munitz, A.M. Bamberger, S. Wannaparhun, R. Abbaschin, J. Mater. Sci. 41 (2006) 2749–2759.
[21] Z. Xie, H. Gao, H. Lu, Z. Wang, B. Sun, J. Alloys Compd. 508 (2010) 320–323.
[22] Z.W. Wu, J.J. Liu, Y. Chen, L. Meng, J. Alloys Compd. 467 (2009) 213–218.
[23] B.B. Straumal, B. Baretzky, A.A. Mazilkin, F. Philipp, O.A. Kogtenkova, M.N. Volkov, R.Z. Valiev, Acta Mater. 52 (2004) 4469–4478.
[24] B.B. Straumal, S.G. Protasova, A.A. Mazilkin, E. Rabkin, D. Goll, G. Schultz, B. Baretzky, R.Z. Valiev, J. Mater. Sci. 47 (2012) 360–367.
[25] S.I. Hong, M.A. Hill, H.S. Kim, Metall. Mater. Trans. A 31 (2000) 2457–2462.
[26] D. Raabe, S. Ohsaki, K. Hono, Acta Mater. 57 (2009) 5254–5263.
[27] D.E. Porter, G.E. Easterling, Phase Transformations in Metals and Alloys, second ed., Chapman and Hall, London, 1993.
[28] B. Sun, H. Gao, J. Wang, D. Shu, Mater. Lett. 61 (2007) 1002–1006.
[31] W.A. Spitzig, Scr. Metall. 23 (1989) 1177–1180.